Construction and Building Materials 150 (2017) 903–915

Contents lists available at ScienceDirect

Construction and Building Materials

journal homepage: www.elsevier.com/locate/conbuildmat

Effect of reinforcement on shrinkage stresses in timber members

Philipp Dietsch

Technical University of Munich, Germany

HIGHLIGHTS

- Indication of necessary reduction of timber moisture content leading to critical stresses with respect to shrinkage cracking.
- Explanation of cracking pattern – one large crack instead of small, evenly distributed cracks.
- Proving the advantage of applying inclined reinforcement in timber members prone to shrinkage.
- Guidance values for equilibrium moisture content of timber members in different types of use.

ARTICLE INFO

Article history:
Received 26 March 2017
Received in revised form 23 May 2017
Accepted 5 June 2017
Available online 21 June 2017

Keywords:
Wood
Timber
Glued laminated timber
Reinforcement
Threaded rod
Screw
Moisture
Shrinkage
Swelling
Moisture induced stresses
Cracking

ABSTRACT

Reinforcement in timber members in form of fully threaded screws or threaded rods can restrict the free shrinkage or swelling of the wood material. This paper presents an evaluation of the influence of such reinforcement on the magnitude of moisture induced stresses with emphasis on shrinkage. For this purpose, experimental studies are presented in combination with analytical considerations on the basis of the Finite-Element method. Taking into account the influence of relaxation processes, the results indicate that a reduction of timber moisture content of 3% around threaded rods, positioned perpendicular to the grain, can already lead to critical stresses with respect to moisture induced cracks. Reduction of timber moisture content of 1% can already neutralize the proportionate stress transfer by the reinforcement in the uncracked member. The cracks appear as few but large cracks, a crack distribution, known from reinforced concrete, does not occur. This is explained by the much smaller ratio between stiffness and strength of timber members compared to concrete members. Guidance values for the equilibrium moisture content of reinforced timber members in different types of use are given.

1. Introduction

Changes in wood moisture content lead to changes of virtually all physical and mechanical properties (e.g. strength and stiffness properties) of wood. An additional effect of changes of the wood moisture content is the shrinkage or swelling of the material and the associated internal stresses.

Visualizing the cross-section of a structural timber member reveals that the area near the surface of the member adapts quite quickly to changes in the surrounding climate (temperature, relative humidity). Areas inside the cross-section require a longer time to reach the equilibrium moisture content due to the greater necessary length of moisture transport by diffusion. The distribution of timber moisture content in the cross-section is therefore not only dependent on the relative humidity, but also on time. This results in a moisture gradient across the cross-section.

Changes in timber moisture content result in strains of different magnitude across the timber cross-section due to the associated shrinkage or swelling of the timber. During the drying process of a timber member, the wood material near the surface is restrained by the inner cross-section, comparable to an elastic foundation. This results in tensile stresses perpendicular to the grain near the surface, which are counterbalanced by compressive stresses inside the cross-section due to the necessary equilibrium of stresses, see Fig. 1. These stresses are reduced over time due to relaxation processes. However, if they locally exceed the very low tensile strength perpendicular to grain, the result will be a stress relief in form of cracks, see Fig. 2. These can reduce the load-carrying capacity of structural timber members in e.g. shear or tension perpendicular to grain.

If the free deformation of the cross section is prevented by restraining forces, e.g. fasteners in dowel-type connections, the magnitude of moisture induced stresses depends on the difference between the strains of the timber cross-section and the restraining

E-mail address: dietsch@tum.de

http://dx.doi.org/10.1016/j.conbuildmat.2017.06.033
0950-0618/

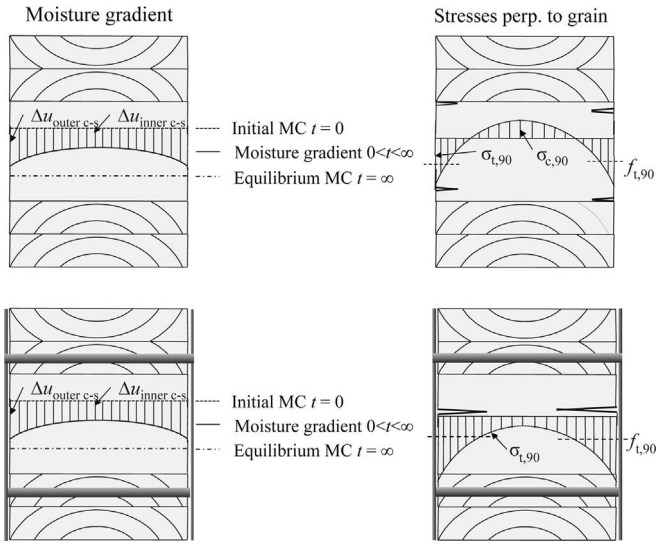

Fig. 1. Schematic illustration of moisture gradient and resulting stresses perpendicular to the grain in case of free shrinkage (above) and in case of restrained shrinkage due to e.g. fasteners (below).

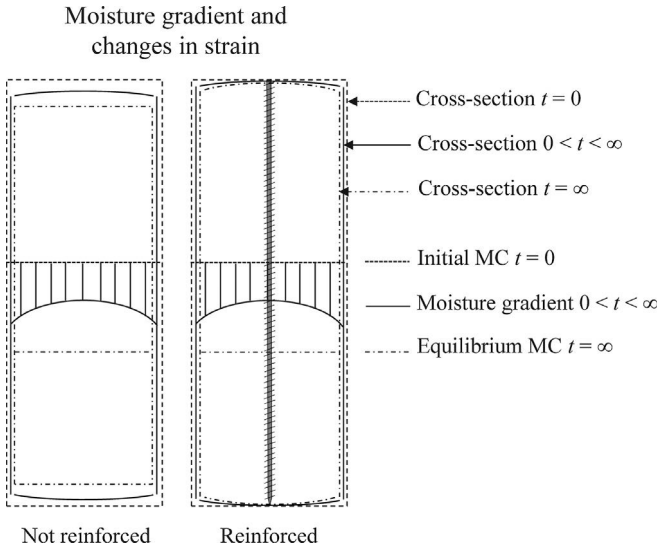

Fig. 3. Schematic illustration of deformed shape of timber cross section under shrinkage, not reinforced (left) and reinforced (right).

elements. Equilibrium of tensile and compressive moisture induced stresses is impeded by the restraining forces. This results in stresses of higher magnitude and eventually in deep shrinkage cracks, see Fig. 1. An example are supports with dowel-type fasteners arranged at considerable vertical distances, see Fig. 2.

Reinforcement of timber members is used to relieve the reinforced members of stresses for which timber only features low strength. Therefore reinforcement, oftentimes applied in form of fully threaded screws or threaded steel rods, is commonly positioned perpendicular to the grain to counter the low corresponding tensile strength of timber. In such a configuration however, the free deformation of the surrounding wood material is restrained due to the semi-rigid composite action between the wood material and the thread of the reinforcement, see Fig. 3. The reason is that steel features an expansion coefficient with respect to temperature but, in contrast to wood, not with respect to changes of moisture. Compared to the temperature expansion coefficient of steel ($\alpha_T = 1.2 \cdot 10^{-6}$/K) are the associated average shrinkage and swelling coefficients of wood perpendicular to the grain (spruce: 0.25%/% Δu) in the order of magnitude of 200 higher. Taking into account common changes in temperature and relative humidity and the reaction of steel, respectively wood to these changes, results in a ratio of approximately 30 between the corresponding expansion of wood and steel.

Fig. 2. Examples of crack formation in glued-laminated timber (glulam) beams in practice. Free shrinkage and rather evenly distributed shrinkage cracks of small depth (left) and deep shrinkage crack between two rows of fasteners (right).

The result observed in practice are few but deep shrinkage cracks, see Fig. 4. Even the full fracture (separation) of the beam cross-section can be observed, resulting in associated stress release in the beam, see Fig. 4. The transfer of released stresses is activated by deformations in the fracture plane. In this example, threaded steel rods were applied as reinforcement of holes in beams positioned in vicinity of the beam ends. The damage scenario shown in Fig. 4 can be explained by the superposition of moisture induced tensile stresses perpendicular to the grain with stress peaks due to the geometry of the hole in combination with high shear stresses due to the location close to the beam end, leading to a fully developed crack through the hole including shear displacement in the fracture plane.

In the following, a mechanical model to describe abovementioned situation is presented and discussed. Based on this model, an experimental setup is derived. Experimental results obtained with this setup are introduced into a Finite-Element model to derive indications on critical reductions of moisture content (MC) in glued-laminated timber (glulam) elements reinforced with fully threaded screws or threaded rods. Numerical analysis is then extended to typically reinforced forms of glulam beam found in practice. The results are compared to timber moisture contents measured via long-term monitoring in buildings of different types of use.

2. Mechanical model

The considerations given in the following refer to dowel-type steel reinforcement such as fully threaded screws or pre-drilled,

Fig. 4. Examples of crack formation in glued-laminated timber (glulam) beams reinforced with threaded steel rods positioned perpendicular to the grain. Deep shrinkage crack (left, photo credits: Brunauer) and crack over full cross-section, leading to shear displacement in fracture plane (right).

screwed-in or glued-in threaded steel rods, placed perpendicular to the grain in the center of the timber cross-section. These considerations can be translated to reinforcement in form of wood-based panels, attached to the edges of the cross-section. To describe such reinforced cross sections mechanically, a beam on elastic foundation in longitudinal direction can be used, see Fig. 5. The stiffness of the semi-rigid composite action is represented by the embedment modulus (modulus of foundation) in longitudinal direction. In the case of a timber member under shrinkage, the result will be compressive trajectories in conical form around the ends of the reinforcement. Perpendicular thereto, tensile stress trajectories will develop which will subsequently align parallel to the reinforcement, see Fig. 5. The magnitude of moisture induced stresses depends on the difference between the strains of the timber cross-section and the restraining elements.

Considering the behavior of the bond between the wood structure and the reinforcement, three mechanisms are considered: adhesion, mechanical interlock and friction. All three mechanisms are activated during a relative displacement between the wood material and the reinforcing element. Adhesion is only existent in the case of glued-in reinforcement, its properties are dependent on the characteristics of the adhesive. In the case of screwed-in reinforcement, the stress transfer is realized by mechanical interlock between the wood material and the thread of the reinforcement. This results in local compressive stresses around the thread which are counterbalanced by tensile stresses that develop in circular form around the reinforcement. In [1] analytical solutions are derived for the situation of a rod in timber under different loading conditions.

3. Experiments

3.1. Configuration of experiments

Two approaches are possible with respect to an experimental investigation of crack formation due to restrained shrinkage or swelling of a timber member with interior reinforcement. The first obvious approach is long-term experiments on reinforced timber members in a climate chamber. This approach was applied in [2–5]. The climate cycles applied in [2,3] led to high moisture gradients, making it difficult to differentiate between crack formation due to the moisture gradient or crack formation due to the predrilled, screwed-in respectively glued-in threaded steel rods restraining free shrinkage. Preliminary calculations show that, in order to arrive at a reduction of moisture of Δu = -5% in the interior of a cross-section of b = 140 mm at a maximum permissible moisture gradient of Δu_{grad} = 2%, a drying period of almost one year is necessary. Since neither climate chambers nor measuring equipment were available for this period, it was decided to pursue another approach.

The second approach is based on the idea that, in the case of a relatively stiff composite between the threaded steel reinforcement and the wood material, the type and location of the induced strains have a rather small effect on the stress distribution in the timber member. Using the mechanical model given above, and assuming either exterior load (e.g. tensile force on the reinforcement) or internal stresses (e.g. restrained shrinkage), the main transfer of stresses between the steel reinforcement and the wood material will occur in the vicinity of both ends (x = 0, x = ℓ) of the steel reinforcement, see Fig. 6. This means that, although the nature of the strain (shrinkage strain or strain due to externally applied tensile load) is different from one another, the stress distribution in the timber member, resulting from the interaction between the wood material and the glued-in or screwed-in threaded steel reinforcement, is comparable.

To validate this assumption, both types of loading were implemented in a Finite-Element-Model. The detailed description of the computational model, the chosen parameters and the assumptions taken are given in Section 4. In this model, a constant change in moisture content was applied to a non-reinforced glued-laminated timber (glulam) element (b / h = 200 / 1000 mm^2), and to the same glulam element being reinforced with a steel rod (d = 16 mm, E_{bond} = 3000 N/mm^2, d_{bond} = 1 mm). The resulting difference in deformation between both configurations was subsequently applied as positive strain on the steel rod in the glued-laminated timber (glulam) element. Fig. 7 shows the corresponding vertical deformations and stresses perpendicular to the grain (vertical stresses) in both configurations. The assumption of comparable stress distribution is not fully valid in the direct vicinity of the steel rod, but appropriate outside this localized area extending between 20 mm and 50 mm. The stress peaks around the ends of the steel rod decrease significantly over a short distance, i.e. crack formation and stress redistribution will remain locally confined. With respect to crack formation in building practice, areas are of relevance in which distinct stresses occur over a significant volume. This is the case around the axis of inertia of the glulam element. The distribution of vertical stresses on the outer edge of the cross-section indicates that a perceptible crack formation will mostly likely occur within the inner quarters of the element height. Within this area, the stress distribution is similar for both types of loading. Based on these findings it was decided to carry out short-term experiments on real-size specimens. It should be noted that time-dependent effects occurring in practice have to be considered when evaluating the results.

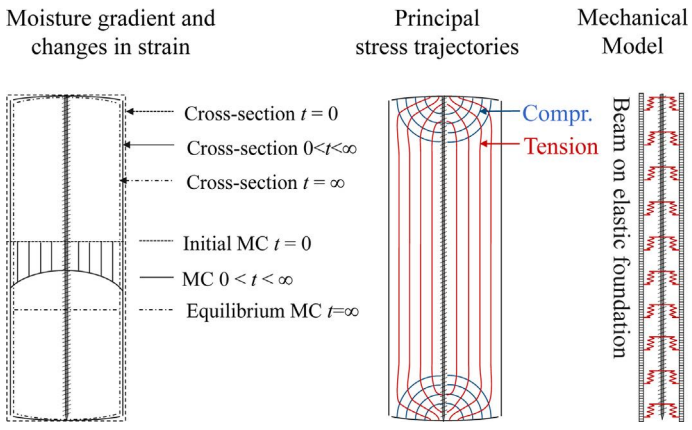

Fig. 5. Schematic illustration of deformed shape, principal stress trajectories and mechanical model of a reinforced timber cross section under shrinkage.

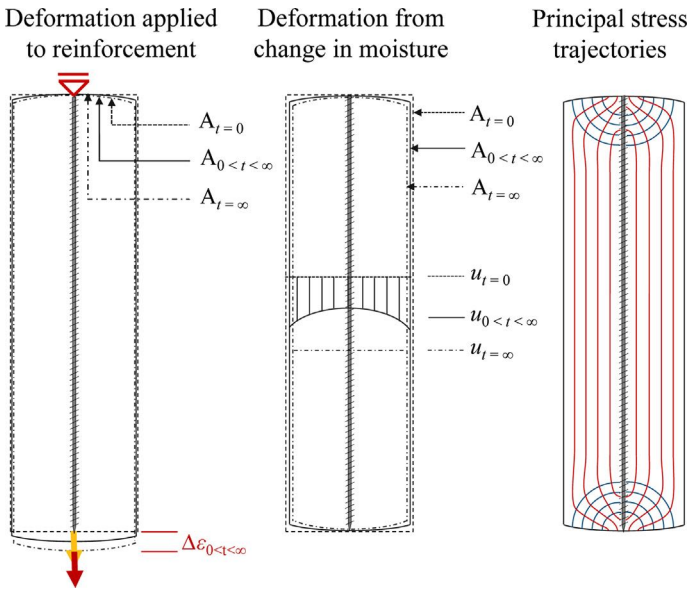

Fig. 6. Schematic illustration of deformation in dependence of type of loading (exterior load or moisture change) and resulting principal stress trajectories.

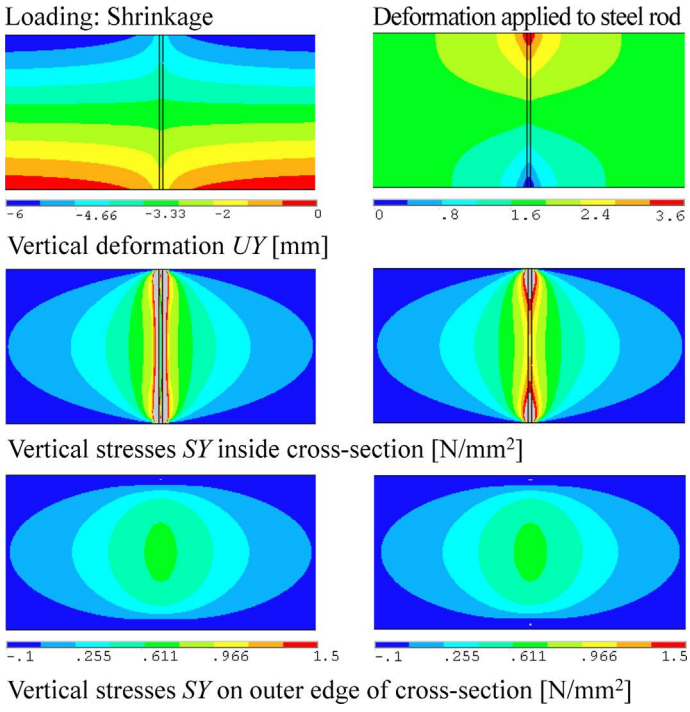

Fig. 7. Distribution of vertical deformation and stresses perpendicular to the grain (vertical stresses SY, normalized, in [N/mm^2]) in a reinforced glued-laminated timber (glulam) element at different types of loading (left: shrinkage; right: exterior load on steel rod).

3.2. Material, specimen characteristics and test procedure

Fig. 8 shows the geometry and dimensions of the test specimens. The two glued-laminated timber (glulam) specimens (No. 1 and No. 2) were made from spruce lamellas (d = 40 mm), using PRF glue. According to the product marking, the lamellas were machine-graded, the strength class was glulam GL24c. According to [6], the strength an stiffness properties relevant for these experiments ($f_{t,90,k}$; E_{90}) are similar for homogeneous ("h") and combined ("c") glulam. The specimens featured a density of $\rho_{12\%,no.1}$ = 423 and $\rho_{12\%,no.2}$ = 416 kg/m^3, mean year-ring width of 4 mm and mean moisture contents of $u_{no.1}$ = 9.8% and $u_{no.2}$ = 10.0%. The maximum difference in moisture content between a depth t = 10 mm and t = 50 mm, measured with the resistance method and isolated electrodes at different depths, was Δu = 0.7%. The difference in specimen length (ℓ_1 = 500 mm, ℓ_2 = 300 mm,) originated from the objective to evaluate different arrangements (spacings) of the threaded steel rods. After completion of the first test series, the length of both specimens was reduced to ℓ = 100 mm for a second test series. Threaded steel rods M16 x 2500 [mm] - 8.8 featuring a metric thread and positioned perpendicular to the grain were glued into the specimens using

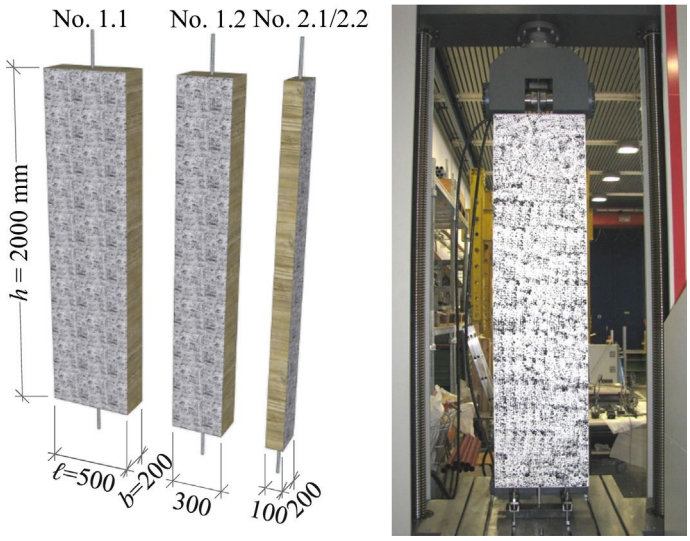

Fig. 8. Geometry of test specimens (left) and specimen with black-and-white pattern in testing machine (right).

Epoxy glue ($d_{glueline}$ = 2 mm). The maximum eccentricity between the glued-in steel rods and the axis of inertia was e = 30 mm.

The tests were realized as displacement controlled tensile tests, whereby the tensile load was applied to the glued-in steel rods at a rate of 1.5 mm/min, measuring load and crosshead travel along the way. In addition, the strain distribution at the surface of the specimens was recorded by means of a contact-free optical measurement system (Aramis) at a frequency of 1 Hz. Utilizing two cameras featuring 5 megapixel, a calibration tolerance of 0.04 in combination with the measured area of 2000 mm yields a measuring tolerance of 0.03 mm or ε = 0.0015%. A stochastic black-and-white pattern was applied to the specimens surface for adequate contrast, see Fig. 8.

3.3. Results

The load–displacement diagram for all experiments is given in Fig. 9. All tests showed linear-elastic behavior. Above a load of F = 110 kN, the threaded steel rod showed plastic deformation. During the first test run (No. 1.1), a U-profile used for clamping the specimen at the bottom began to deform plastically above a load of 60 kN, resulting in a vertical deformation of 7 mm at the end of the test. In the first test (1.1), a small vertical drop can be noticed at F = 107 kN and u = 10.7 mm, which also appears during the second test (1.2) at F = 99 kN and u = 7.4 mm, see Fig. 9. Both drops in load level mark the sudden appearance of one visible and continuous crack. A further load-increase led to the opening of the existing crack but not to the development of additional cracks. The absence of such a vertical drop in the load-deformation curves of the second test series indicates that no further cracks appeared during this test series.

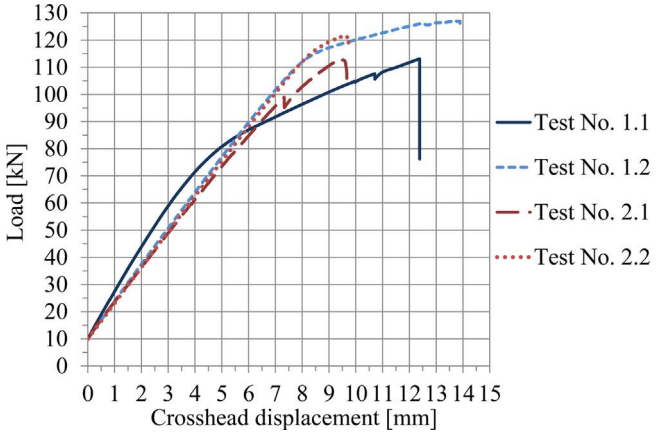

Fig. 9. Load-displacement diagram.

Fig. 10 shows the strain distribution on test specimen 1.1 at different load levels. It shows a slow and local crack formation and the sudden development into a continuous crack at a load of F = 107 kN. At this load level, the local maximum strains reached $\varepsilon_{max} \approx 0.5\%$. Apparent is the inhomogeneous strain distribution as well as the considerable stress relief above and below the continuous crack. The fact that no additional cracks formed during the second test series could also be deduced from the absence of areas of small strains above or below an area of large strains. For more comprehensive documentation beyond this paper, the interested reader is referred to [7] for the strain distributions of the additional tests.

4. Numerical modelling and analytical considerations

4.1. Model assumptions and modelling of experiments

To assess the stress distribution in the specimens, the experimental configuration was modelled and computed using a commercially available Finite-Element program (ANSYS) with 3-D volume elements featuring mid-nodes. Since the objective was to receive a general overview, a linear-elastic material model was implemented. In the computational model, the stiffness parameters of the specimens were varied until the increase in deformation at the surface equaled the average linear increase in deformation measured for a load increase of 10 kN during the experiments. The only stiffness parameters that became relevant under given type of loading were the modulus of elasticity perpendicular to the grain, E_{90}, and - to a limited extent - the rolling shear modulus, G_r. Both feature a considerable dependence on the orientation of the growth rings (radial vs. 45° vs. tangential), see [8–11]. Since most lamellas featured an orientation of growth rings between 30° and 60°, an increased rolling shear modulus G_r = 150 N/mm^2 was applied, see [11]. All other stiffness parameters of the glulam specimens for strength grade GL24c were taken from [12]. Stiffness and cross-section of the threaded steel rod were not varied since

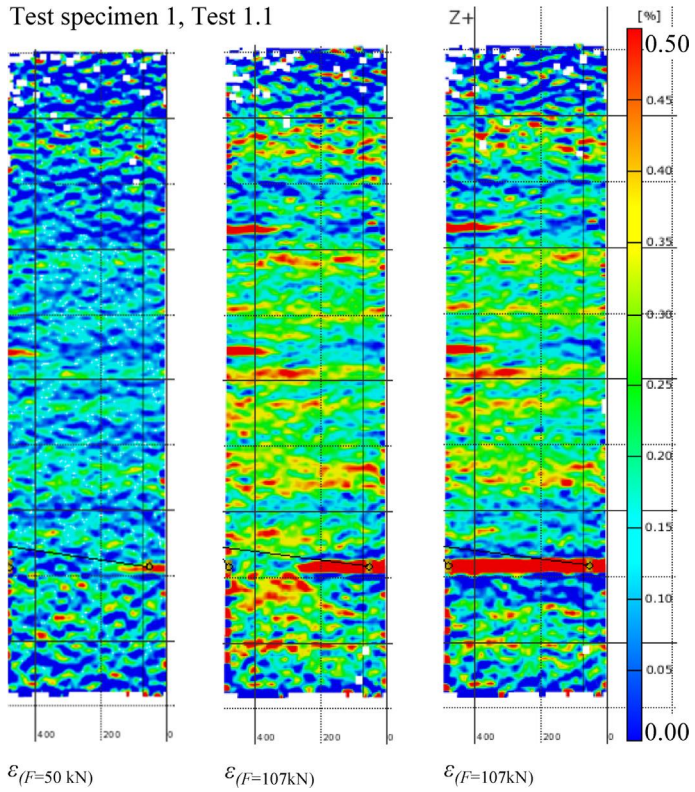

Fig. 10. Strain distribution ε [–] of test specimen 1.1 at F = 50 kN and directly before and after the formation of a continuous crack (lower quarter at F = 107 kN).

their variation is very low. The bond stiffness was taken as $E = 3000\ N/mm^2$ see [13,14]. Varying geometry and stiffness parameters of the bond within realistic bounds showed only marginal influence on the magnitude of strains and stresses in the glulam specimens. Applying abovementioned assumptions yielded mean moduli of elasticity perpendicular to the grain of $E_{90,mean,no.1} = 250\ N/mm^2$ and $E_{90,mean,no.2} = 320\ N/mm^2$. The value determined for specimen 1 seems low at first sight. However, a comparison with values determined by [9] for the same geometry of lamellas ($190 \leq E_{90,mean} \leq 395\ N/mm^2$) shows that this value is realistic. The changes in timber moisture content were implemented through a change in temperature of the material. The shrinkage and swelling coefficients for spruce perpendicular to the grain ($\alpha_r = 0.16\%/\%\Delta u$, $\alpha_t = 0.32\%/\%\Delta u$) were implemented as an averaged coefficient of thermal expansion ($\alpha_{90} = 0.24\%/\%\Delta T$). A more detailed description of the model, parameters used and further assumptions can be found in [7].

4.2. Results and evaluation of results

After implementation of abovementioned assumptions and parameters in the Finite-Element-model, the mean tensile stresses perpendicular to the grain were determined for the load at fracture and at maximum load, F_{max}. Using the same model, the equivalent decrease in moisture content, causing a corresponding distribution and magnitude of tensile stresses perpendicular to the grain was determined. Table 1 contains the values derived for all test specimens. Taking into account the dependence of the tensile strength perpendicular to the grain on the stressed volume, the results fit well the values given in [9,15].

With respect to a realistic estimation of equivalent changes in timber moisture content until crack formation it is of great importance to take into account the relaxation of timber during shrinkage and swelling processes. Research works on this subject have identified values of stress relaxation due to mechano-sorptive effects in the range of 40% - 60%, see e.g. [16–18]. In [19], even higher values are determined. In building practice, dowel-type steel such as fully threaded screws or pre-drilled, screwed-in or glued-in threaded rods, is mostly placed in the center of the cross-section. Due to the decelerated adaption of timber moisture content in the center, relaxation values will presumably establish in the upper range of abovementioned values.

Assuming a relaxation of 50%, the resulting equivalent (constant) reduction in timber moisture content is $\Delta u_{equiv,no.1} = -3.1\%$ and $\Delta u_{equiv,no.2} = -2.6\%$.

Table 1
Mean tensile stresses perpendicular to the grain and equivalent reduction of timber moisture content.

Specimen	$\sigma_{t,90,mean}$ at crack [N/mm^2]	u_{equiv} [%] (without relaxation)	$\sigma_{t,90,mean}$ at F_{max}[N/mm^2]
1.1 (ℓ = 500 mm)	0.48	−1.4	0.51
2.1 (ℓ = 300 mm)	0.60	−1.2	0.68
1.2 (ℓ = 100 mm)			0.83
2.2 (ℓ = 100 mm)			0.98

4.3. Explanation of observed crack pattern

During the experiments, only one continuous crack appeared. Even though the Finite-Element-model of the second test series yielded tensile stresses perpendicular to the grain that locally exceed the stresses at crack formation during the first test series by up to 70%, no further crack formation was detected during the second series. A crack distribution, known from reinforced concrete structures under shrinkage, did not occur. One explanation can be derived from the "theory of the weakest link" (e.g. [20,21]) according to which the crack appears at the location of

lowest strength. The stresses subsequently distribute to areas of higher strength. At the same time, the areas of load transfer between the steel reinforcement and wood material increase, meaning that the areas of high stresses in the timber member decrease. An additional effect is the very inhomogeneous structure of the wood material in combination with the very heterogeneous distribution of strength-reducing factors like knots, ring shake and resin pockets. This can explain why - apart from the area of initial crack formation - no further area featured strength below the tensile stresses perpendicular to the grain that occurred after crack formation and during the second test series, see Fig. 11.

To answer the question why a crack distribution, known from reinforced concrete structures under shrinkage, does not occur, two prerequisites have to be taken into account. The first factor, necessary for equal crack distribution, is a homogeneous distribution of strength and stiffness properties in the area considered. Both materials feature coefficients of variation of approximately 20% with respect to modulus of elasticity (perpendicular to the grain) and approximately 30% for tensile strength (perpendicular to the grain), whereby locally much higher variations can occur [9,22,23]. The second prerequisite is a high ratio between strength and stiffness of the material to achieve a fast load transfer at small deformation in direct vicinity of the crack. This is the case for concrete, whereas for wood perpendicular to the grain, this ratio is about 27.5 times smaller.

$$\frac{E_{cm,C30/37}/f_{ctk;0.05,C30/37}}{E_{90,mean,GL}/f_{t,90,k,GL}} = \frac{33,000/2.0}{300/0.5} = \frac{27.5}{\underline{\underline{1}}} \quad (1)$$

In addition it has to be taken into account that reinforcing elements, placed in the center of a timber cross-section feature a material cover (edge distance to surface) which is between two to five times higher than the typically applied concrete cover [23]. Combining these arguments it can be explained why the restraining forces, induced by the reinforcing elements during shrinkage processes, do not lead to a distribution of relief cracks.

4.4. Modelling of configurations with relevance to building practice

Using the Finite-Element-model described above, different types and configurations of reinforced glued-laminated timber (glulam) members that find application in building practice, were modelled to gain additional information on the distribution and magnitude of moisture induced stresses due to restricted shrinkage or swelling of the glulam member. The parameters were implemented as upper and lower bounds of practical relevance, e.g. element height h_{min} = 1.0 m, h_{max} = 2.0 m. Material parameters were taken from European Standards [6] and Technical Approvals [14], the latter for bond stiffness for glued-in threaded steel rods (E = 3000 N/mm^2). For screwed-in threaded rods, few experimental results exist [3,24]. The results, however, are not fully in agreement due to different approaches in deformation measurement. The results are also limited to screwed-in lengths of $\ell \leq 400$ mm, necessitating extensive extrapolation. In addition, the test results represent the load-case pull-compression (pulling the threaded steel rod while holding the glulam specimen). This load-case is applicable for cracked, reinforced glulam members as the stresses released in the crack can be assumed to act as one single load on the steel rod. The transfer of stresses between the threaded steel rod and the uncracked glulam member is less represented by this test configuration. A better suited test method is presented in [25,26], however test results for screwed-in threaded steel rods determined with this test method are not yet available. Due to the high uncertainty of the bond stiffness of screwed-in threaded rods of larger length in uncracked glulam members it was decided to not explicitly model this case but to evaluate the influence of bond stiffness via randomly chosen steps of stiffness. If not explicitly stated, the change in timber moisture content was taken as Δu = -2.5%. Moisture gradients were not modelled since the objective was to enable a separate consideration of the two phenomena.

The first analysis shown in the following is reduced to the model featuring h = 1000 mm, reinforced by steel rods. Since such reinforcement can either be used as reinforcement against tensile stresses perpendicular to the grain or shear stresses, angles between steel rod and grain direction of 90° and 45° were implemented. In the following, the results of the model featuring a bond stiffness of E = 3000 N/mm^2 (comparable to a glued bond) are presented.

Fig. 12 shows the distribution of stresses perpendicular to the grain (vertical stresses) in a glued-laminated timber (glulam) element, reinforced with one steel rod at angles of 90° and 45°. The distribution for the model featuring a steel rod placed at 90° corresponds with the stress trajectories resulting from the mechanical model (Fig. 5). The cone of tensile stresses around the steel rod is axisymmetric to the principal direction of the reinforcement.

In case of a steel rod placed at 45°, the stress distribution is point symmetric with respect to the center of gravity of the reinforcement. This stress distribution can be explained by the decreasing cross-section of the glulam element due to shrinkage, forcing the steel rod into an S-shape. This leads to tensile stresses perpendicular to the grain between the steel rod and

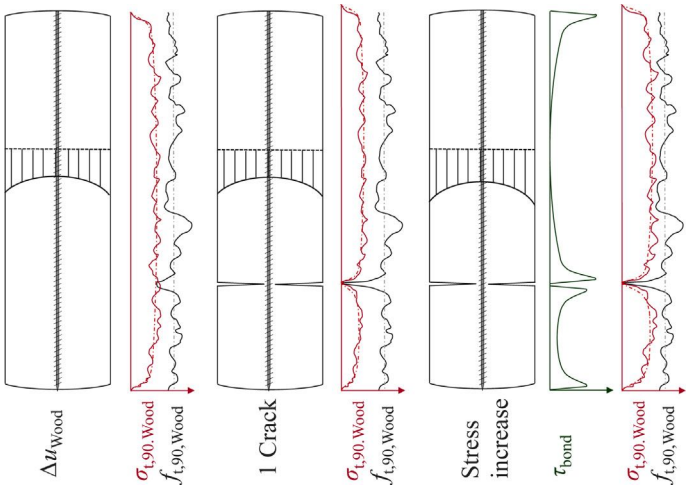

Fig. 11. Scheme of distribution of tensile stresses and strength perpendicular to the grain (and resulting crack formation) in case of variable strength and stiffness properties.

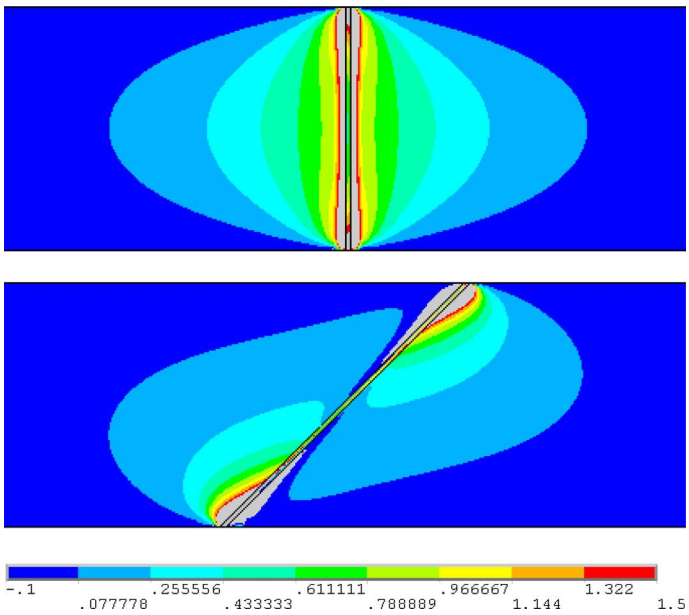

Fig. 12. Distribution of stresses perpendicular to the grain (vertical stresses, normalized, in [N/mm^2]) in glued-laminated timber (glulam) element, reinforced with one steel rod at angles of 90° (above) and 45° (below).

the longitudinal axis of inertia of the glulam element. A detailed comparison between both configurations shows that the tensile stresses perpendicular to the grain can, at certain limited locations, reach the same magnitude. In the configuration with a steel rod placed under 45°, the volume under stress is reduced to about 15%, when compared to the configuration with a steel rod placed at 90°.

In practice, the number of necessary reinforcing elements and their spacing is dependent on the area to be reinforced, the magnitude of stresses therein and the maximum and minimum permissible spacing between the reinforcing elements. With respect to reinforcement against tensile stresses perpendicular to the grain in curved beams it is recommended in [27] to choose spacing between $a_{1,min} = 250$ mm and $a_{1,max} = 0.75\ h_{max}$. For shear reinforcement, possible spacing is discussed in [7], but official technical guidance is not yet available.

The following two Figures (Fig. 13 with the results for an angle of 90°, Fig. 14 with the results for the configuration at

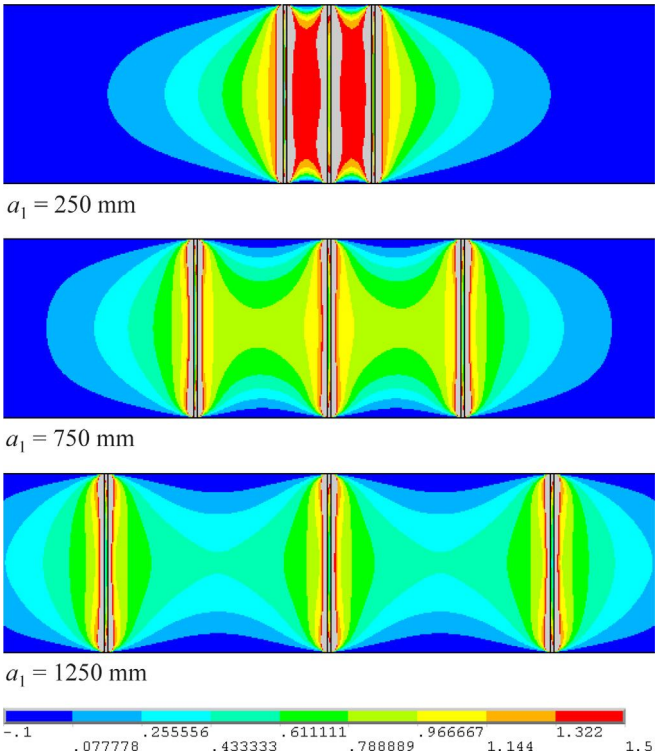

Fig. 13. Distribution of stresses perpendicular to the grain (vertical stresses, normalized, in [N/mm^2]) in glued-laminated timber element, reinforced with steel rods at different spacing, angle 90°.

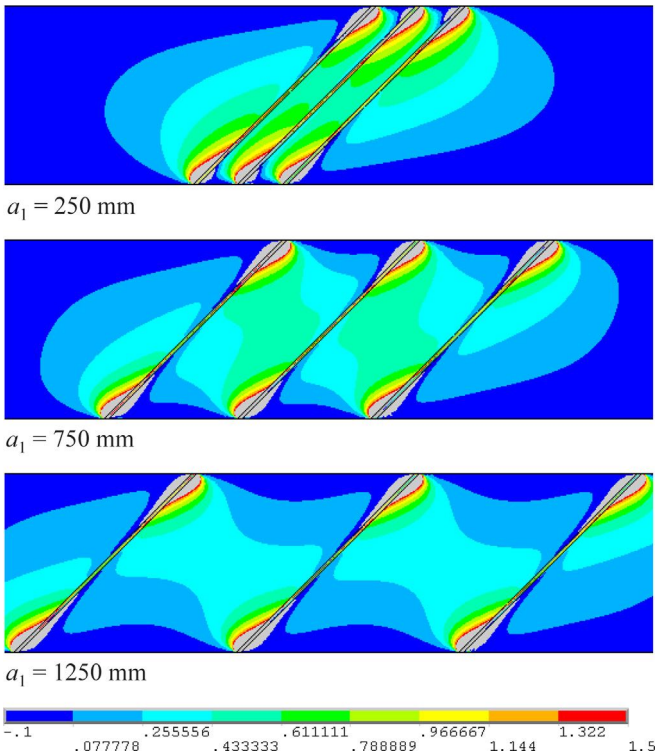

Fig. 14. Distribution of stresses perpendicular to the grain (vertical stresses, in [N/mm^2]) in glued-laminated timber element, reinforced with steel rods at different spacing, angle 45°.

45°) show the distribution of stresses perpendicular to the grain (vertical stresses) in a glulam element, reinforced with glued-in steel rods at spacings $a_1 = 250$ mm, $a_1 = 750$ mm and $a_1 = 1250$ mm (= 1.25 h). As expected, increased spacing leads to a reduction of interaction. However, even in the configuration featuring the largest spacing between the steel rods, an interaction is still apparent. Steel rods placed at 90° to grain direction lead to a higher interaction and therefore to a larger increase in stresses perpendicular to the grain, in comparison to the configuration featuring steel rods at 45°. A detailed comparison between both configurations shows that the magnitude of stress peaks is independent of the configuration. Outside these localized areas, the stresses for the configuration at 45° are about 45% lower than for the configuration at 90°.

With each step of increased spacing ($a_1 = 250$, 750, 1250 mm), the stresses reduce by 40 – 45%, whereby the proportion of magnitude of stresses remains constant between both configurations. A considerable reduction of bond stiffness ($E = 3000 \rightarrow 100$ N/mm^2) led to a reduction of stresses of 10 – 15%. Increasing the bond stiffness had no influence on the magnitude of stresses.

4.5. Modelling of reinforced glulam beams used in building practice

To receive more information on the implication of aforementioned effects for building practice, it was decided to model reinforced curved and pitched cambered glulam beams. Such beams are frequently applied in timber engineering practice since their geometry can follow the desired form of the roof and their changing depth offers the possibility to adapt the section modulus to the bending moment (however leading to the opposite effect for shear), see Fig. 15. The curvature leads to deviation forces, resulting in tensile stresses perpendicular to the grain for which timber features very small capacities [6]. Therefore the curved part is typically reinforced against tensile stresses perpendicular to the grain by means of pre-drilled, screwed-in or glued-in threaded steel rods.

The FE-program used and model parameters were similar to those described in Section 4.4 with the exception that the reinforced beams were modelled as plane elements to reduce computation time, i.e. stiffness parameters and change of moisture content were assumed constant over the beam width. One objective (not further evaluated in this paper) was to evaluate the proportionate distribution of tensile stresses perpendicular to the grain between the glulam beam and the reinforcement. This depends on factors such as spacing between the threaded steel rods, bond stiffness and curvature of the beam. The second objective was to determine at which reduction of moisture content, the proportionate transfer of tensile stresses perpendicular to the grain from curvature is neutralized by adverse moisture induced tensile stresses perpendicular to the grain from restraining forces imposed by the reinforcement. The beam chosen for illustration of the results is a curved beam with length $\ell = 20$ m, width $b = 180$ mm, height at support $h_A = 1230$ mm, height at apex $h_{ap} = 1400$ mm, angle of upper beam edge (= angle of roof), $\delta = 15°$, angle of lower beam edge, $\beta = 13°$, angle of taper, $\alpha = \delta - \beta = 2°$, radius of curvature $r_{in} = 20$ m. Fig. 16 shows the tensile stresses perpendicular to the grain in the curved part of the beam, fully reinforced with glued-in steel rods at spacings 1000 mm $\leq a_1 \leq$ 1250 mm along the length of the curvature and loaded only with different reductions of moisture content Δu, assuming a relaxation of 50%.

It can be seen that the stresses increase proportionally with increasing reduction of timber moisture content. The highest stresses occur around the steel rods, between the steel rods, the stresses slightly decrease, an interaction of stresses is apparent. The mean tensile stresses perpendicular to the grain in the neutral axis of the inner part of the curvature at a reduction of timber moisture content $\Delta u = -3\%$ are slightly below $\sigma_{t,90} = 0.50$ N/mm^2 (including an assumed relaxation of 50%).

In the next step the beams were loaded with a uniformly distributed load such that the maximum design bending stresses matched the design bending resistance. Fig. 17 shows the tensile stresses perpendicular to the grain in the neutral axis of the curved beam reinforced with glued-in steel rods under different reductions of moisture content Δu and under different extent of reinforcement.

It can be observed that the reinforcement reduces the tensile stresses perpendicular to the grain in the curved part of the glulam beam from $\sigma_{t,90} = 0.35$ N/mm^2 to about $\sigma_{t,90} = 0.20$ N/mm^2, i.e. to approximately 60% of the stresses in the unreinforced beam. A reduction in timber moisture content of $\Delta u = -1\%$ neutralizes this reinforcing effect as it leads to moisture induced tensile stresses perpendicular to the grain in the same order of magnitude. The corresponding stress distribution containing both superposing effects reaches approximately the same magnitude as the stress

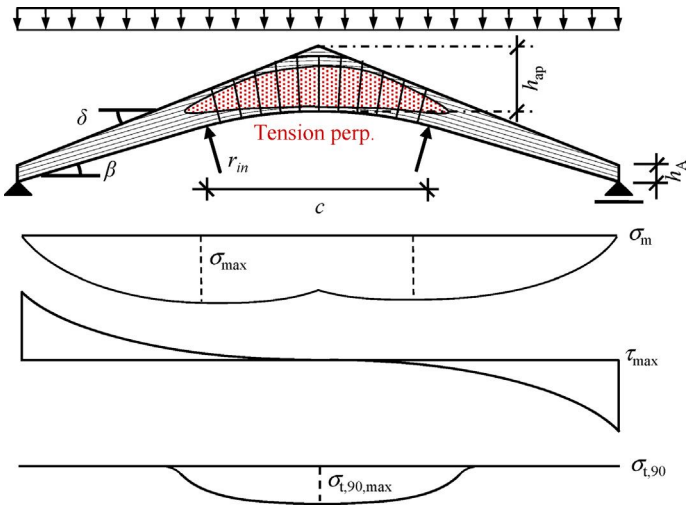

Fig. 15. Schematic illustration of the distribution of bending stresses, shear stresses and tensile stresses perpendicular to the grain and arrangement of corresponding reinforcement with threaded steel rods in pitched cambered beam.

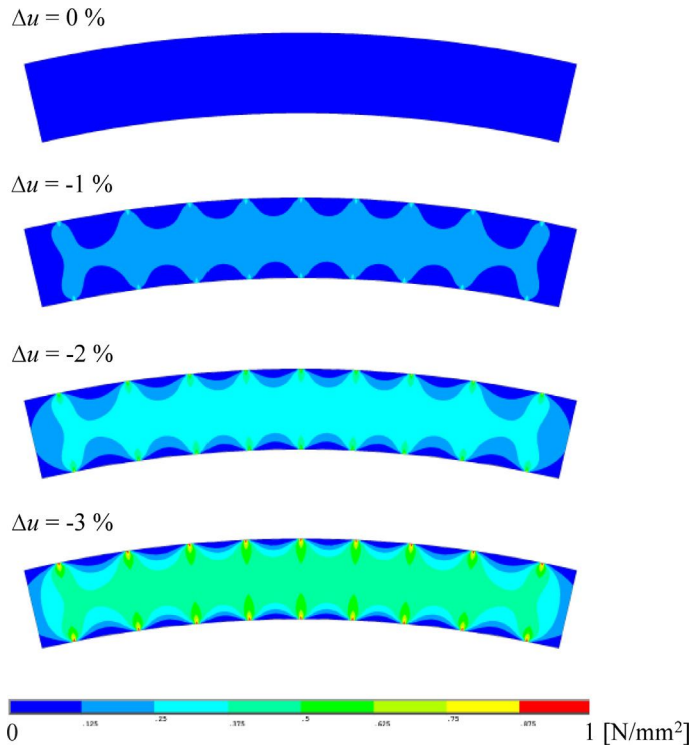

Fig. 16. Tensile stresses perpendicular to the grain (in [N/mm^2]) in curved part of unloaded glued-laminated timber beam fully reinforced with glued-in steel rods under different reductions of moisture content u, Figure based on [28].

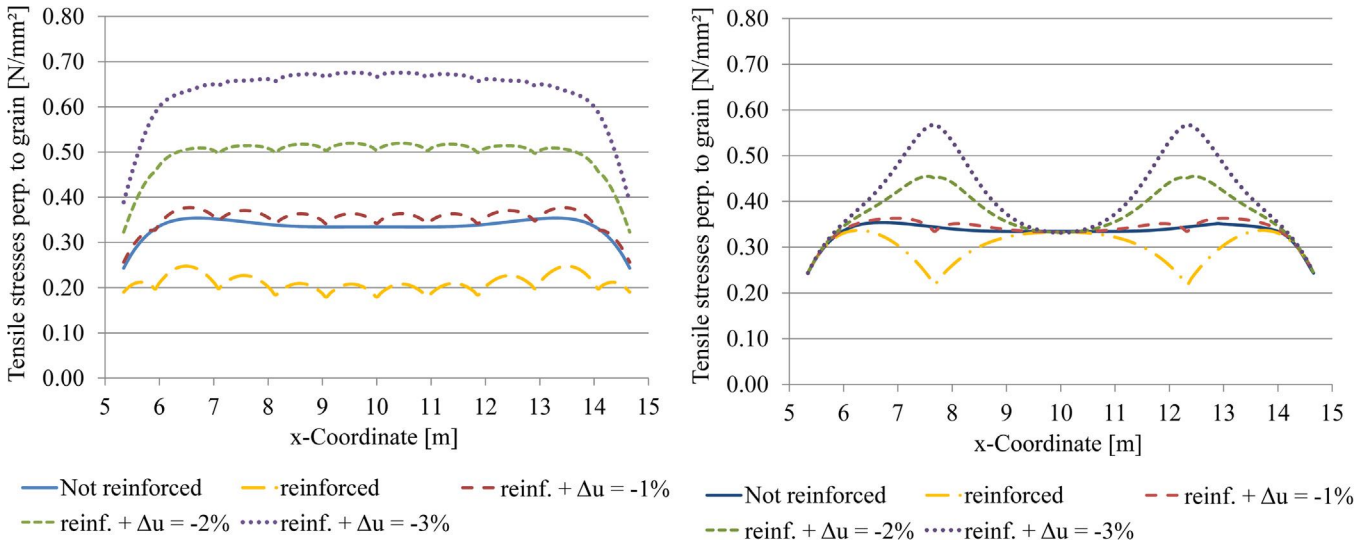

Fig. 17. Tensile stresses perpendicular to the grain (in [N/mm^2]) in neutral axis of uniformly loaded curved glued-laminated timber beam reinforced with glued-in steel rods under different reductions of moisture content u, full reinforcement (left), reduced reinforcement (right), Figure based on [28].

distribution for the unreinforced case. A further reduction in timber moisture content results in higher tensile stresses perpendicular to the grain as in the unreinforced beam.

The observed effects are relatively independent of the chosen quantity of reinforcement and its type of bond (glued-in or predrilled and screwed-in). This can be explained by the fact that quantity and bond type have the same effect on both phenomena: the proportionate transfer of tensile stresses perpendicular to the grain in the curved part of uncracked glulam beams (lower for screwed-in compared to glued-in steel rods, see above) as well as inducing tensile stresses perpendicular to the grain when restraining the free shrinkage and swelling. To evaluate the effect of beam geometry, ten representative geometries of curved and pitched cambered beams were modelled. These were given four different types of reinforcement, glued-in and screwed-in steel rods, once at smaller spacing to carry the full tensile stresses perpendicular to the grain and once at larger spacing to carry a portion of the tensile stresses perpendicular to the grain. For these forty configurations, the reduction in timber moisture content Δu was determined at which the reinforcing effect is neutralized in the

neutral axis of the curved part of the uncracked beam. The resulting values Δu are within -0.7% $\leq \Delta u \leq$ -2.6 (Δu_{mean} = 1.5%). The influencing factor is the radius of curvature (modelled radii 7.5 m $\leq r_{in} \leq$ 25 m), implicitly determined by the angle of the lower beam edge, β, and the length of the curved part, c, see Fig. 15. A small radius will lead to higher stresses perpendicular to the grain. The higher corresponding strains lead to a higher activation of the steel rods (activation by deformations), implying that higher strains from restrained shrinkage are necessary to neutralize the reinforcing effect. The length along the curved part at which the influence of the steel rod have fully diminished varied between $2.6 \cdot h_{ap} \leq a_{100} \leq 3.2 \cdot h_{ap}$ (a_{100} as total length, i.e. to both sides of the steel rod). The length at which the tensile stresses perpendicular to the grain induced by one steel rod reduce to 25% of the stresses in direct vicinity of the steel rod was determined to $1.5 \cdot h_{ap} \leq a_{75} \leq 1.6 \cdot h_{ap}$.

5. Timber moisture contents in building practice

Reinforcement against tensile stresses perpendicular to the grain in form of fully threaded screws or pre-drilled, screwed-in or glued-in threaded steel rods is common practice in large-span timber structures, e.g. to counter tensile stresses perpendicular to the grain from deviation forces in curved beams. The moisture content of such members in use is dependent on the surrounding climate which is again influenced by the use of the building. Here it is possible to roughly group into: insulated and heated buildings featuring a rather constant, mostly dry climate, e.g. sport halls (gymnasiums), swimming pools, production, sales facilities and sheltered, non-insulated and unheated buildings featuring periodic changes of surrounding climate, e.g. riding rinks, agricultural buildings, warehouses.

Within a research project [29], surrounding climate and timber moisture content were monitored in 21 buildings from 7 different types of use. Tables 2 and 3 contain indicative mean values and timber moisture contents, u, their annual amplitudes, max. A (at 15 mm depth), mean temperatures, T, and mean relative humidity, rh. In insulated and heated buildings the average moisture content was in the range of 6%–10% with annual amplitudes of 2%. In sheltered, non-insulated and unheated conditions, the moisture content was in the range of 12–16% with annual amplitudes of 4%.

With respect to moisture induced tensile stresses perpendicular to the grain from reinforcement restraining the free shrinkage of the wood material, timber members in buildings featuring a constant but dry climate (i.e. buildings falling into Table 2) are more critical. The reason is that reinforcement in form of fully threaded screws or pre-drilled, screwed-in or glued-in threaded steel rods is typically arranged in the middle of the member cross-section, i.e. periodic changes of surrounding climate are less critical when regarding the interior parts of the timber cross-section (edge distance of 70 mm or more).

Although timber design standards such as [30] require that "before being used in construction, timber should be dried as near as practicable to the moisture content appropriate to its climatic condition in the completed structure", most timber products are produced and delivered at moisture contents 10% $\leq u \leq$ 12%. In the research project [29], mean timber moisture contents as low as u = 5% were measured in specific locations (in sunlight, below skylights, at ventilation outlets, above machines). Comparing these to timber moisture contents during production and erection, the potential effect of the singular but strong drying of a timber member in such a magnitude becomes obvious.

6. Conclusions

The reaction of wood to moisture forms an integral part of any task in connection with this natural and renewable building material. With respect to reinforcement, this poses the question of its influence on the magnitude of moisture induced stresses, since reinforcement restricts the free shrinkage or swelling of the timber member. For this purpose, experimental studies (short-term tests) were carried out in combination with analytical considerations on the basis of the Finite-Element method. The numerical model used contains assumptions and uncertainties, the results however should enable to indicate an order of magnitude.

Taking into account the influence of relaxation processes, the results indicate that a reduction of timber moisture content of 3% around threaded steel rods, positioned perpendicular to the grain, can already lead to critical tensile stresses perpendicular to the grain with respect to moisture induced cracks. Reductions of timber moisture content of 1% can already neutralize the proportionate stress transfer by the reinforcement in the uncracked member.

Table 2
Indicative values for the monitored insulated and heated buildings during normal use, derived from data of the entire measurement period [29].

Category	Timber MC		Temperature	rel. humidity
	mean [%]	max. A [%]	mean [°C]	mean [%]
Swimming Pools	8.5	1.5	30	<50
Gymnasiums (sports facilities)	8–10	2	20	<50
Production and sales	6.5	<2	20	<50
Ø Insulated and heated	6 – 10	≤2	≥20	<50

Table 3
Indicative values for the partially open, non-insulated and non-heated buildings during normal use, derived from data of the entire measurement period [29].

Category	Timber MC		Temperature	rel. humidity
	mean [%]	max. A [%]	mean [°C]	mean [%]
Riding rinks	16	4	12	>75
Agricultural facilities (livestock)	15	4	13	70
Warehouses	12	4	11	60–75
Ø Non-insulated, non-heated	12 – 16	4	12	>65

The shrinkage cracks appear as few but large cracks, a crack distribution, known from reinforced concrete, does not occur. This is explained by the much smaller ratio between stiffness and strength of timber members compared to concrete members and the larger distance between the reinforcement and the member surface. These results indicate that reinforcing elements like predrilled, screwed-in or glued-in threaded steel rods should be placed in the center of the timber cross-section. Periodic, e.g. yearly changes of surrounding climate have a smaller influence on timber moisture content in the interior of a cross-section. Permanent change of timber moisture content will lead to a slower adaption of the same in the interior of a cross-section, enabling relaxation processes to unfold over a longer period. Due to the heterogeneous distribution of stiffness properties across the width of one lamella, tensile stresses perpendicular to the grain from exterior loads will be highest in the center of the cross-section. Finally, a placement in the center of the timber cross-section is more robust with respect to potential deviation of the drill hole during production. If multiple rows of reinforcement are necessary, e.g. in block-glued members, an adequate edge distance should be ensured. Until more experience is gained, an edge distance of at least 70 mm is proposed.

In case of reinforcement with 45° inclination, the magnitude of moisture induced stresses is reduced to about half while the stressed volume is reduced even more (to about 15%). Therefore the conclusion is to apply reinforcement at an inclination. This is especially true in areas of high shear stresses (close to beam ends, at notches and holes in beams) as an inclination would reduce the risk of full cracking of the beam, which would release the shear stresses and at the same time enable proportionate transfer of the same. In case of doubt about the potential magnitude of shrinkage, inclined reinforcement should be designed to carry both, the tensile stresses perpendicular to the grain as well as the shear stresses.

For both types of arrangement, a substantial mutual influence of adjacent reinforcing elements could be identified. A reduction of the spacing between the reinforcing elements thus results in a lower tolerable reduction of timber moisture content around the reinforcement. Therefore the aim should be to realize larger spacings between reinforcing elements and reducing the height of the reinforced areas in the timber member.

Before being reinforced and used in construction, timber should be dried as near as practicable to the moisture content appropriate to its climatic condition in the building in use. Additional measures include a coordinated construction regime (e.g. preventing wetting during prolonged storage, reduction of unnecessary construction moisture). In dry use environments, controlled drying of the timber to service conditions should be planned. Reinforcement of timber members to be exposed to dry climate should be designed to carry the full stresses under consideration. Reinforcement to carry only a portion of the tensile stresses perpendicular to the grain, as e.g. given in [27], should not be applied in dry conditions as a potential stress release in form of shrinkage cracks due to restrained free shrinkage of the timber member could lead to a safety problem. A robust alternative is external plane reinforcement in form of plywood or laminated veneer lumber that is glued onto the entire surface area under tensile stresses perpendicular to the grain as such reinforcement decelerates the process of moisture changes or drying of the timber member. In addition, the smaller ratio of stiffness between the reinforcement and the timber member results in lower moisture induced stresses from restrained shrinkage. Hence such reinforcement may be favourable in applications with permanently dry climate.

This publication examines a rather recent field of research, hence more experience in form of experimental as well as numerical studies would be beneficial. Experimental investigations should include long-term tests in climate chambers on reinforced timber members subjected to realistic climate scenarios (changes of relative humidity in realistic time intervals). This objective is being pursued within a recently started research project at the Chair of Timber Structures and Building Construction (TUM). In the field of numerical studies, additional knowledge could be gained from modelling of experiments as well as configurations used in practice, focussing on the dependency of strength and stiffness parameters on annual ring patterns.

Acknowledgements

Part of this work was carried out in the frame of the authors' dissertation. The invaluable suggestions and support from Prof. Heinrich Kreuzinger is highly acknowledged. Gratitude is extended to Prof. Stefan Winter for his helpful and constructive supervision as well as to Prof. Hans Joachim Blaβ for his interest in my work and many interesting discussions. The students Andreas Denig and Michael Probst are thanked for their contributions in the frame of their study paper respectively Master thesis.

References

[1] P.J. Gustafsson, E. Serrano, Glued-in rods for timber structures – development of a calculation model. Report ISRN LUTVDG/TVSM - 01/3056 - SE(l-96), Lund University, 2001.
[2] J. Ehlbeck, P. Belchior-Gaspard, M. Gerold, Eingeleimte Gewindestangen unter Axialbelastung bei Übertragung von großen Kräften und bei Aufnahme von Querzugkräften in Biegeträgern – Teil 2: Einfluß von Klimaeinwirkung und Langzeitbelastung 1992 Abt. Ingenieurholzbau, Universität Karlsruhe Forschungsbericht der Versuchsanstalt für Stahl, Holz und Steine.
[3] H.J. Blaß, O. Krüger, Schubverstärkung von Holz mit Holzschrauben und Gewindestangen, Band 15 der Reihe Karlsruher Berichte zum Ingenieurholzbau, KIT Scientific Publishing, Karlsruhe, 2010.
[4] V. Angst, K.A. Malo, Effect of self-tapping screws on moisture induced stresses in glulam, Engi. Struct. 45 (2012) 299–306.
[5] B. Wallner, Versuchstechnische Evaluierung feuchteinduzierter Kräfte in Brettschichtholz verursacht durch das Einbringen von Schraubstangen. Master Thesis. Institute of Timber Engineering and Wood Technology, Graz University of Technology, 2012.
[6] EN 14080:2013. Timber structures - Glued laminated timber and glued solid timber – Requirements. CEN, Brussels, 2013.
[7] P. Dietsch, Einsatz und Berechnung von Schubverstärkungen für Brettschichtholzbauteile Dissertation, Technical University of Munich, 2012.
[8] J. Bodig, B.A. Jayne, Mechanics of Wood and Wood Composites, Van Norstrand Reinhold, New York, 1982.
[9] H.-J. Blaß J. Ehlbeck M. Schmid Ermittlung der Querzugfestigkeit von Voll- und Brettschichtholz. Forschungsbericht, Versuchsanstalt für Stahl und Holz, Abt. Ingenieurholzbau, Universität Karlsruhe, 1998.
[10] J. Jönsson, S. Svensson, A contact free measurement method to determine internal stress states in glulam, Holzforschung 58 (2) (2004) 148–153.
[11] R. Görlacher, Ein Verfahren zur Ermittlung des Rollschubmoduls von Holz, Holz als Roh- und Werkstoff 60 (5) (2002) 317–322.
[12] DIN 1052:2008-12. Entwurf, Berechnung und Bemessung von Holzbauwerken – Allgemeine Bemessungsregeln und Bemessungsregeln für den Hochbau. DIN, Berlin, 2008.
[13] G. Habenicht, Kleben: Grundlagen, Technologien, Anwendungen, 5 Auflage, Springer, Berlin.
[14] DIBt Z-9.1-705. Allgemeine bauaufsichtliche Zulassung, 2K-EP-Klebstoff WEVO-Spezialharz EP 32 S mit WEVO-Wärter B 22 TS zum Einkleben von Stahlstäben in Holzbaustoffe. Deutsches Institut für Bautechnik, Berlin, 2009.
[15] P.J. Gustafsson, Fracture perpendicular to grain – structural applications, in: S. Thelandersson, H.J. Larsen (Eds.), Timber Engineering, Wiley, West Sussex, England, 2003.
[16] K. Möhler, G. Maier, Kriech- und Relaxations-Verhalten von lufttrockenem und nassem Fichtenholz bei Querdruckbeanspruchung, Holz als Roh- und Werkstoff 28 (1) (1970) 14–20.
[17] G. Steck, Abbau von Eigenspannungen aus Feuchteänderungen bei Brettschichtholz durch Sägeschnitte. Forschungsbericht, Versuchsanstalt für Stahl, Holz und Steine, Abt. Ingenieurholzbau, Universität Karlsruhe, 1985.
[18] T. Toratti, S. Svensson, Mechano-sorptive experiments perpendicular to grain under tensile and compressive loads, Wood Sci. Technol. 34 (4) (2000) 317–326.
[19] V. Angst, K.A. Malo, The effect of climate variations on glulam - an experimental study, Eur. J. Wood Wood Products 70 (5) (2012) 603–613.
[20] W. Weibull, A Statistical Theory of the Strength of Materials. Royal Swedish Institute for Engineering Research, Proceedings No. 151, 1939.
[21] J.D. Barrett, Effect of size on tension perpendicular to grain strength of Douglas Fir, Wood and Fiber 6 (2) (1974) 126–143.

[22] EN 1992-1-1:2004 + AC:2010. Eurocode 2: Eurocode 2: Design of concrete structures – Part 1-1: General rules and rules for buildings. CEN, Brussels, 2010.
[23] K. Zilch, G. Zehetmaier, Bemessung im konstruktiven Betonbau, Springer, Berlin, 2010.
[24] H. Stamatopoulos, K.A. Malo, Withdrawal stiffness of threaded rods embedded in timber elements, Constr. Build. Mater. 116 (2016) 263–272.
[25] P. Mestek, S. Winter, Konzentrierte Lasteinleitung in Brettsperrholz-konstruktionen – Verstärkungsmaßnahmen. AiF Forschungsvorhaben Nr. 15892 – Schlussbericht, Lehrstuhl für Holzbau und Baukonstruktion, Technical University of Munich, 2011.
[26] M. Danzer, P. Dietsch, S. Winter, Reinforcement of holes in glulam beams arranged excentrically or in groups, in: Proceedings of the World Conference on Timber Engineering WCTE 2016, Vienna, Austria.
[27] DIN EN 1995-1-1/NA:2013-08, National Annex – Nationally determined parameters – Eurocode 5: Design of timber structures – Part 1-1: General – Common rules and rules for buildings. DIN, Berlin, 2013.
[28] M. Probst, Einfluss von Art und Anordnung von Querzugverstärkungen auf die Abtragung vorhandener Querzugspannungen in Satteldachträgern. Master Thesis, Chair of Timber Structures and Building Construction, Technical University of Munich, 2016.
[29] P. Dietsch, A. Gamper, M. Merk, S. Winter, Monitoring building climate and timber moisture gradient in large-span timber structures, J. Civil Struct. Health Monitoring 5 (2) (2014) 153–165.
[30] EN 1995-1-1:2008, Eurocode 5: Design of timber structures – Part 1-1: General – Common rules and rules for buildings. CEN, Brussels, 2008.